Desalination and Water Treatment
www.deswater.com

doi: 10.1080/19443994.2014.992973

57 (2016) 4548–4556
February

Arsenic removal from contaminated drinking water by electrocoagulation using hybrid Fe–Al electrodes: response surface methodology and mechanism study

Peipei Song[a,b], Zhaohui Yang[a,b,*], Haiyin Xu[a,b], Jing Huang[a,b], Xia Yang[a,b], Feng Yue[a,b], Like Wang[a,b]

[a]*College of Environmental Science and Engineering, Hunan University, Changsha 410082, China, Tel. +86 14726989246; email: songpeipei@hnu.edu.cn (P. Song), Tel. +86 15717484818; email: yzh@hnu.edu.cn (Z. Yang), Tel. +86 13874958492; email: xuhaiyin2006@126.com (H. Xu), Tel. +86 18507315018; email: gavinhj@163.com (J. Huang), Tel. +86 13667360406; email: ceia@hnu.edu.cn (X. Yang), Tel. +86 15116224945; email: 1501847759@qq.com (F. Yue), Tel. +86 15873121768; email: 24759564@qq.com (L. Wang)*

[b]*Key Laboratory of Environmental Biology and Pollution Control, Hunan University, Ministry of Education, Changsha 410082, China*

Received 4 April 2014; Accepted 22 November 2014

ABSTRACT

This study investigated the optimization and mechanism of arsenic (As) removal by electrocoagulation (EC) using hybrid Fe–Al electrodes. Response surface methodology (RSM) was employed to evaluate the effects of different operating conditions on As removal and voltage. Central composite design was established for the optimization of the EC process and to evaluate the effects and interactions of process variables: current density, pH, aeration intensity, and operating time. Analysis of variance showed a high coefficient of determination value ($R^2 = 0.9269$), ensuring a satisfactory adjustment of the second-order regression model with the experimental data. Under the optimum conditions of current density 0.47 A/dm^2, pH 7.0, aeration intensity 0.32 L/min, and operating time 20 min, 99.94% As were removed and the minimum energy consumption was obtained. Results confirmed the validity of the optimization and the adequacy of the model. Besides, scanning electron miscroscopy/energy dispersive spectroscopy, X-ray diffraction, and Fourier transform infrared analysis demonstrated that adsorption onto iron and aluminum hydroxides/oxyhydroxides was the predominant mechanism of As removal by EC using hybrid Fe–Al electrodes.

Keywords: Arsenic; Electrocoagulation; Response surface methodology; Mechanism

1. Introduction

Arsenic (As), a toxic, mutagenic and carcinogenic trace element, poses a great threat to human beings [1]. As can be released into waters by both natural processes and anthropogenic activities, such as weathering of As containing minerals, uncontrolled industrial discharge from mining and metallurgical industries, and abuse of As containing pesticides [2]. As and its compounds negatively affect human health including various skin lesions such as hypopigmentation (white spots), hyperpigmentation (dark spots),

---

*Corresponding author.

and keratosis of hands and feet. They also damage the cardiovascular, gastrointestinal tract, reproductive, and central nervous system even at a low concentration. Long-term exposure to As can also cause cancer of the bladder, lungs, skin, liver, and prostate [3,4]. US Environmental Protection Agency (EPA) and World Health Organization (WHO) have lowered the maximum permissible concentration for As in drinking water from 50 to 10 μg/L [5,6].

There are many techniques of As removal from wastewater such as adsorption, biological process, and chemical coagulation [7–13]. However, these treatment technologies require several pH adjustments as well as addition of acid and coagulants [14,15]. In addition, some processes generate a considerable quantity of secondary pollutants which causes serious environmental problems. Electrocoagulation (EC), an emerging water treatment technology, has been applied successfully to treat various wastewaters, especially, heavy metal contaminated water [16–19].

As removal by EC can be affected by many factors including electrode material, current density, concentration, pH, time, and so on [20–23]. Previous studies indicated that Fe–Al plates as sacrificial electrodes in EC process was very promising for As removal [20,23]. Thus, in this study, As was removed by EC using hybrid Fe–Al electrodes. Our previous study investigated the effects of experiment parameters including current density, aeration intensity, pH, and operating time on As removal. However, it is vitally important to find an adequate experimental design to explore the relationship among influencing factors and the combined effects on As removal and energy consumption. Response surface methodology (RSM), a collection of mathematical and statistical technique, has been found to be a useful method for studying the mutual interaction between the variables and optimizing the variables [24,25].

In this study, we employed RSM to investigate the interactive effects of experimental factors including current density, pH, aeration intensity, and operating time, and to optimize the EC process. Besides, EC products were characterized by scanning electron microscopy/energy dispersive spectroscopy (SEM/EDS), X-ray diffraction (XRD), and Fourier transform infrared (FTIR) to explore the mechanism of As removal by EC using hybrid Fe–Al electrodes.

2. Materials and methods

2.1. Materials

All of the chemicals used in this study were of guaranteed reagent (GR) grade. A stock synthetic solution of 1,000 mg/L As was prepared according to the EPA standard method by dissolving As_2O_3 in a solution containing 20% (w/v) KOH, neutralizing with 20% (v/v) H_2SO_4 to a phenolphthalein end point, and then diluting to 1,000 mL with 1% (v/v) H_2SO_4. Simulated wastewaters containing 500 μg/L As were prepared by diluting the above stock solution. All the solutions were prepared with ultrapure water and desired volumes of stock solutions. The sample solution was adjusted to the desired pH with 5% (v/v) HCl and 1 mol/L NaOH. Experiments were carried out in a 4 L reactor. Four plates were vertically positioned in monopolar mode. The submerged surface area of each electrode was 120 cm^2.

2.2. RSM experimental design

The central composite design (CCD), a standard RSM, was selected for optimization of the factors which had great effects on As removal. In this design, four factors (current density, pH, aeration intensity, and time) were investigated. Experimental runs were carried out in triplicates. The independent variables range and levels were set by Design-expertV8.0.6 (Stat-Ease Inc., USA; Table 1). Results of the central points were used to check the reproducibility of results as per CCD. Analysis of variance (ANOVA) was used for graphical analyses of the data to obtain the interaction between the process variables and the responses. The quality of the fit polynomial model was checked by the determination of coefficient (R^2), and its statistical significance was checked by the Fisher F-test in the same program. Model terms were evaluated by the p value (probability) with 95% confidence level. The response variable that represented removal efficiency was fitted by a second-order model in the form of quadratic polynomial equation:

$$y = \beta_0 + \sum_{i=1}^{m} \beta_i \chi_i + \sum_{i<j}^{m} \beta_{ij} \chi_i \chi_j + \sum_{i=1}^{m} \beta_{ii} \chi_i^2 \tag{1}$$

where y is the response variable to be modeled, χ_i and χ_j are the independent variables which determine y, β_0, β_i, and β_{ii} are the offset term, i and j are the linear coefficient and the quadratic coefficient, respectively. β_{ij} is the term that reflects the interaction between χ_i and χ_j [24,25].

2.3. Analysis

EC products were characterized by SEM (Quanta 200 FEG, FEI, Hillsboro, OR). The elemental composition of EC products was performed by EDS. XRD

Table 1
Coded levels for four variables framed by CCD

Factors	Name	Units	Low	High	Minimum	Maximum
A	Current density	A/dm^2	0.47	0.82	0.30	1
B	pH		5	9	3.00	11.00
C	Aeration intensity	L/min	0.16	0.48	0.00	0.64
D	Time	min	10	20	5.00	25.00

analysis of the EC products was carried out with a Bruker D8 diffractometer operating with a Cu Kα radiation source filtered with a graphite monochromator ($\lambda = 1.54058$ Å). The samples were ground to a fine powder and loaded into a sample holder. Powder specimens were filtered with 400-mesh sieves preceding the XRD analysis. The XRD scans were recorded from 10° to 80° 2θ with 0.020° step-width and 6 s counting time for every step-width. FTIR analysis was carried out by FTIR 8400S IR prestige-21 spectrometer using potassium bromide pellets. The spectra were recorded in the range of 4,000–400 cm^{-1} with 2 cm^{-1} resolution, and 32 scans were collected for each specimen. As concentrations were measured by the atomic fluorescence spectrophotometry (AFS) (Haiguang AFS-9760, Beijing) [26].

3. Results and discussion

3.1. Experiments results

Experiments were carried out according to the experimental conditions designed by RSM (Table 2) and the results are presented in both surface and contour plots. Fig. 1 showed the combined effects of four variables on As removal efficiency. It can be ascertained from Fig. 1(a)–(c) that As-removal efficiency increased with the increase in current density. It could be attributed to that at higher current density, the increased anodic metals dissolution (Faraday's law, Eq. (2)) caused an accumulation of hydroxide cationic complexes, leading to higher As-removal efficiency [16].

$$C_{\text{theo}} = \frac{It_{\text{EC}}M}{ZFV} \tag{2}$$

where C_{theo} (g/m^3) is the theoretical amount of ion produced by current I (A) passed for a period of time (s), Z is the number of electrons involved in the oxidation/reduction reaction. M is the atomic weight of anode material, F is the Faraday's constant (96,485 C/mol) and V is the volume (m^{-3}) of the treated water. With the increase in current density, coagulant dosage rate increased. Besides, current density determines growth of flocs which can influence As-removal efficiency [7]. Hence, As-removal efficiency increased with the increase in current density.

It has been well established that pH is an important parameter and has significant influence on EC process. pH was reported to effect the species distribution and the surface charge of As or metal oxides generated in EC process [20,23,27]. Fig. 1(a) and (e) indicated that As-removal efficiency increased from pH 3 to 5 and decreased when pH was above 7. The optimum pH was observed at 5.0–7.0. According to Wan et al. [27], at pH 5.0–7.0, the surfaces of the particles generated in EC process were positively charged and electrostatic contributions as well as chemical contributions contributed to As removal [27]. At pH 3.0–5.0, Fe^{2+}, Fe^{3+}, Al^{3+}, and OH^- ions generated by electrodes reacted to form various monomeric and polymeric species that finally transformed into insoluble iron and aluminum hydroxides/oxyhydroxides through complex polymerization. Above pH 7.0, the highly soluble monomeric anion $Fe(OH)_4^-$ and $Al(OH)_4^-$ concentration increased at the expense of $Fe(OH)_3$ and $Al(OH)_3$ (s) [23].

With the increase in aeration intensity, more and more As(III) were converted into As(V). From Fig. 1(b), (d) and (f), higher As-removal efficiency was obtained at higher aeration intensity. As demonstrated by the previous studies [22,27,28], the predominant specie of As(III) existed as a neutral molecule of H_3AsO_3, while As(V) was mainly in the form of $H_2AsO_4^-$ and $H_2AsO_4^-$. Due to electrostatic attraction and chemical contributions, As(V) removal was usually faster than As(III). Moreover, under aeration conditions, Fe^{2+} was oxidized into Fe^{3+} whose capacity to form hydrate was stronger than Fe^{2+}. Furthermore, aeration provided the necessary turbulent current conditions for the flocs to contact and collide, ultimately resulting in higher As-removal efficiency.

RSM was aimed to evaluate the relationship between four independent variables and responses. It was established well with the quadratic regression model as follows:

Table 2
A full factorial design for four variables along with responses

Factor 1	Factor 2	Factor 3	Factor 4	Response 1	Response 2
A: Current density (A/dm^2)	B: pH	C: Aeration intensity (L/min)	D: Time (min)	As removal efficiency (%)	U (V)
0.65	11	0.32	15	97.02	4.28
0.47	5	0.16	10	69.66	3.20
0.47	9	0.48	20	99.57	3.53
0.47	5	0.16	20	97.44	3.08
0.65	7	0.32	15	99.47	4.26
0.82	9	0.16	20	99.98	5.14
0.47	9	0.16	20	94.21	3.23
0.65	7	0.32	15	98.47	4.18
0.47	9	0.16	10	78.55	3.34
0.82	5	0.16	10	75.79	5.04
0.82	5	0.16	20	97.56	4.91
0.30	7	0.32	15	99.25	2.25
0.82	5	0.48	20	99.47	5.32
0.47	5	0.48	20	94.57	3.15
0.82	9	0.16	10	79.76	5.20
0.65	7	0	15	68.32	4.05
0.47	9	0.48	10	82.34	3.72
0.82	9	0.48	20	99.83	5.13
0.65	7	0.64	15	99.24	4.27
1.00	7	0.32	15	99.98	6.26
0.65	7	0.32	25	99.58	4.18
0.65	7	0.32	15	99.81	4.72
0.65	7	0.32	15	99.75	4.28
0.65	3	0.32	15	98.79	5.04
0.47	5	0.48	10	97.27	3.26
0.65	7	0.32	5	81.08	4.29
0.82	9	0.48	10	99.29	5.29
0.65	7	0.32	15	99.69	4.29
0.65	7	0.32	15	99.72	4.36
0.82	5	0.48	10	99.47	5.38

$$\begin{aligned} Y_1 = {} & 100.00 + 1.13 \times \mathrm{A} - 0.38 \times \mathrm{B} + 6.00 \times \mathrm{C} + 6.24 \\ & \times \mathrm{D} + 0.60 \times \mathrm{A} \times \mathrm{B} + 0.43 \times \mathrm{A} \times \mathrm{C} - 1.35 \times \mathrm{A} \\ & \times \mathrm{D} - 3.10 \times \mathrm{B} \times \mathrm{C} + 0.50 \times \mathrm{B} \times \mathrm{D} - 4.70 \times \mathrm{C} \times \mathrm{D} \\ & - 0.11 \times \mathrm{A}^2 - 0.48 \times \mathrm{B}^2 - 4.07 \times \mathrm{C}^2 - 2.47 \times \mathrm{D}^2 \end{aligned} \tag{3}$$

$$\begin{aligned} Y_2 = {} & 4.29 + 0.95 \times \mathrm{A} - 0.011 \times \mathrm{B} + 0.084 \\ & \times \mathrm{C} - 0.052 \times \mathrm{D} \end{aligned} \tag{4}$$

where Y is the predicted response (Y_1: As-removal efficiency (%); Y_2: voltage (V)), and A, B, C, D are the coded values of current density, pH, aeration intensity, and operating time, respectively.

In order to ensure the adequacy of employed model, an adequate fit of the model should be given to avoid poor or ambiguous results. The significance of quadratic regression model was tested by the value of F, p, and correlation coefficient. The corresponding results of ANOVA are displayed in Table 3. F-value of 13.59 and p value < 0.0001 implied that the model was significant. Values of "Prob > F" less than 0.0500 indicated model terms were significant. In this case C, D, BC, CD, C^2, and D^2 were significant model terms. "Adeq Precision" measured the signal-to-noise ratio. There was only a 0.01% chance that a "Model F-Value" this large could occur due to noise. The ratio of this model was 11.314, an adequate signal. Besides, R^2 was 0.9269, which indicated that this model could be used to navigate the design space. A significant lack of fit implied that there may be some systematic variation unaccounted for in the hypothesized model. The lack of fit was good for the model. Based on these results, the response surface model constructed in this study was considered reasonable [24,25,28].

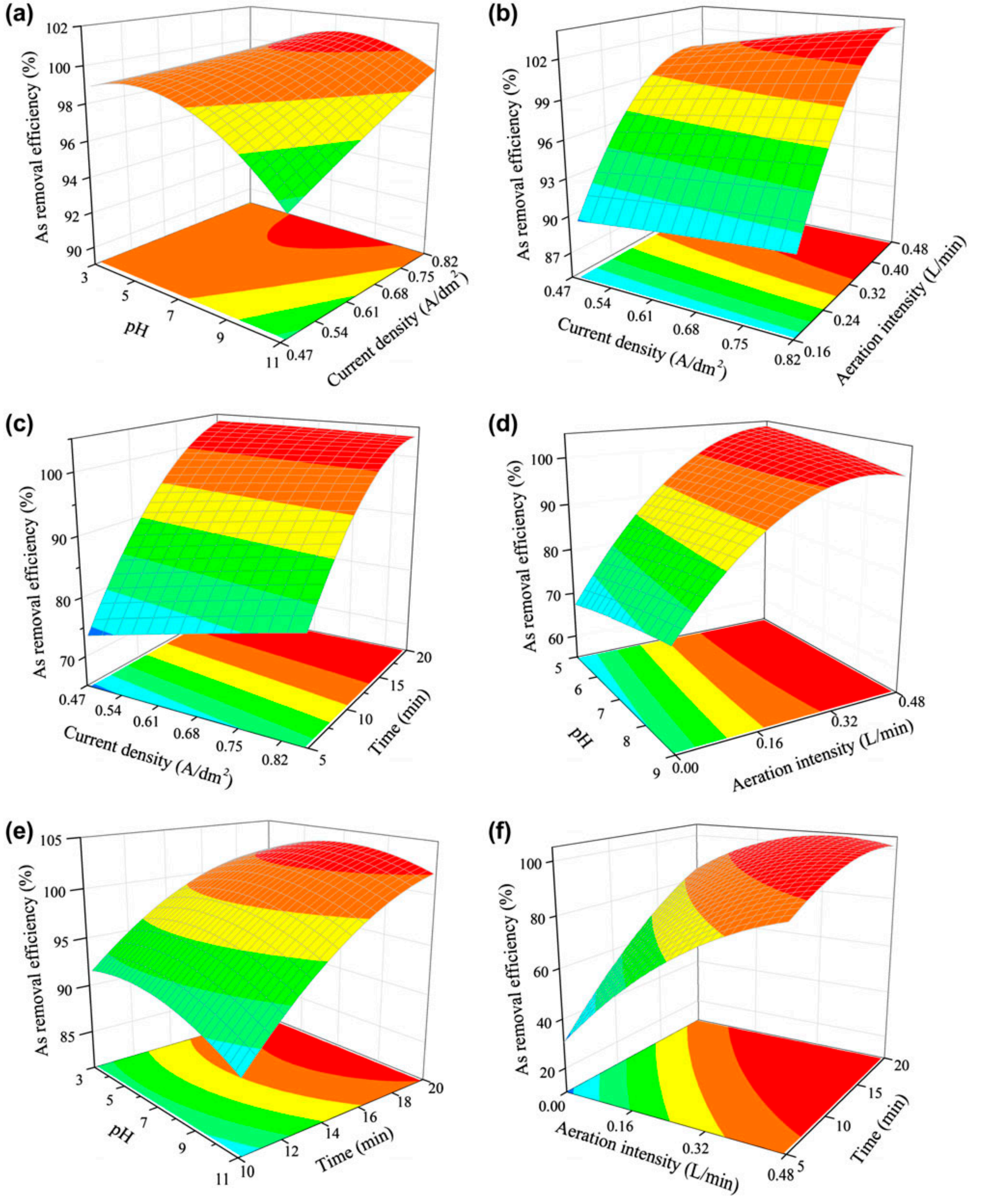

Fig. 1. 3D response surface graphs for combined effects on As removal efficiency. (a) Effects of pH and current density, (b) Effects of current density and aeration intensity, (c) Effects of current density and time, (d) Effects of pH and aeration intensity, (e) Effects of pH and time, and (f) Effects of aeration intensity and time.

Table 3
ANOVA for response surface quadratic model

Source	Sum of Squares	Mean square	*F*-value	p-value, Prob > *F*
Model	2865.97	204.71	13.59	<0.0001
A—Current density (A/dm^2)	30.45	30.45	2.02	0.1756
B—pH	3.45	3.45	0.23	0.6394
C—Aeration intensity (L/min)	862.75	862.75	57.27	<0.0001
D—Time (min)	934.23	934.23	62.02	<0.0001
AB	5.84	5.84	0.39	0.5429
AC	3	3	0.2	0.6615
AD	29.19	29.19	1.94	0.1842
BC	70.73	70.73	4.7	0.0468
BD	3.94	3.94	0.26	0.6164
CD	352.73	352.73	23.42	0.0002
A^2	0.31	0.31	0.02	0.8881
B^2	6.28	6.28	0.42	0.5283
C^2	453.31	453.31	30.09	<0.0001
D^2	167.46	167.46	11.12	0.0045
Residual	225.96	15.06		
Lack of fit	225.96	22.6		
Pure error	0	0		

3.2. Optimization of the EC process for As removal

The main objective of the optimization was to determine the optimum values of variables from the model obtained using experimental data. In optimization, the response of As-removal efficiency was chosen to the maximum value, the response of voltage was chosen to the minimum value and the variables of current density, pH, aeration intensity and time were selected to be within range. The optimization results were current density: 0.47 A/dm^2; pH 7.0; aeration intensity: 0.32 L/min; and time: 20 min. To confirm the model adequacy and the validity of the optimization procedure, additional experiments were performed under the predicted optimal conditions. As a result, 99.94% As were removed and the voltage of 3.23 V was obtained. As concentration remaining in treated waters were far lower than the permissible level of WHO. Compared with other works, EC using hybrid Fe–Al electrodes under the optimum conditions in this study exhibited great potential for As removal as shown in Table 4 [20,29,30]. Validation experiments conducted under the optimal parameters were in agreement with the predicted value. It is evident that the model of RSM is adequate for prediction of As removal by EC using hybrid Fe–Al electrodes. Based on typical electricity cost and material price in China, the operating cost was estimated to be 0.4793 CNY per m^3 of treated water (\$ 0.0782/m^3 with a currency conversion of 6.129 CNY per USD).

3.3. Mechanism involved in As removal

SEM image (Fig. 2(a)) displayed the presence of ultrafine particular structure at μm size. EDS proved the existence of Fe, Al, and As in EC products, which confirmed that As was removed from the solution.

The possible mechanism of As removal includes precipitation, co-precipitation, and adsorption [31]. In this study, precipitation is used in a general way to describe any process resulting in the production of solids [32]. Coprecipitation is defined as an incorporation of soluble As species into a growing hydroxide phase via inclusion, occlusion, or adsorption [31,32]: (1) Inclusion includes two forms: isomorphic inclusion and nonisomorphic inclusion. In isomorphic inclusion, the impurity is substituted into the crystal lattice for a lattice ion of similar size and chemical characteristics. In nonisomorphic inclusion, the impurity appears to be dissolved in the precipitate. (2) In occlusion, an impurity differing in size or chemical characteristics from the lattice sites as the crystals are growing, producing crystal imperfections. (3) In adsorption, the impurity is not incorporated into the internal crystal structure, but rather the formation of surface complexes between soluble species and solid (hydroxide, in this case) surface sites occurs.

If the precipitate mechanism occurs in As removal, As-Fe(III)/Al precipitates should be discovered. However, XRD and FTIR analysis (Fig. 2(c), (d) and Table 5) indicated that no As-Fe(III)/Al precipitates,

Table 4
Comparison of the operational conditions of As removal by EC

Operational conditions						
Electrode	Initial con.	Current density	Aeration intensity (L/min)	Time (min)	As removal efficiency (%)	Reference
Ti	2 mg/L	2.19 mA/cm^2	0	60	58	[26]
Al	13.4 ppm	30 mA/cm^2	0	60	97.8	[18]
Fe	90 μg/L	1.1 mA/cm^2	0	60	97.93	[29]
Fe–Al	1.42–1,230 ppm	30 mA/cm^2	0	60	78.9–99.6	[18]
Fe–Al	500 μg/L	0.47 A/dm^2	0.32	20	>99.94	This study

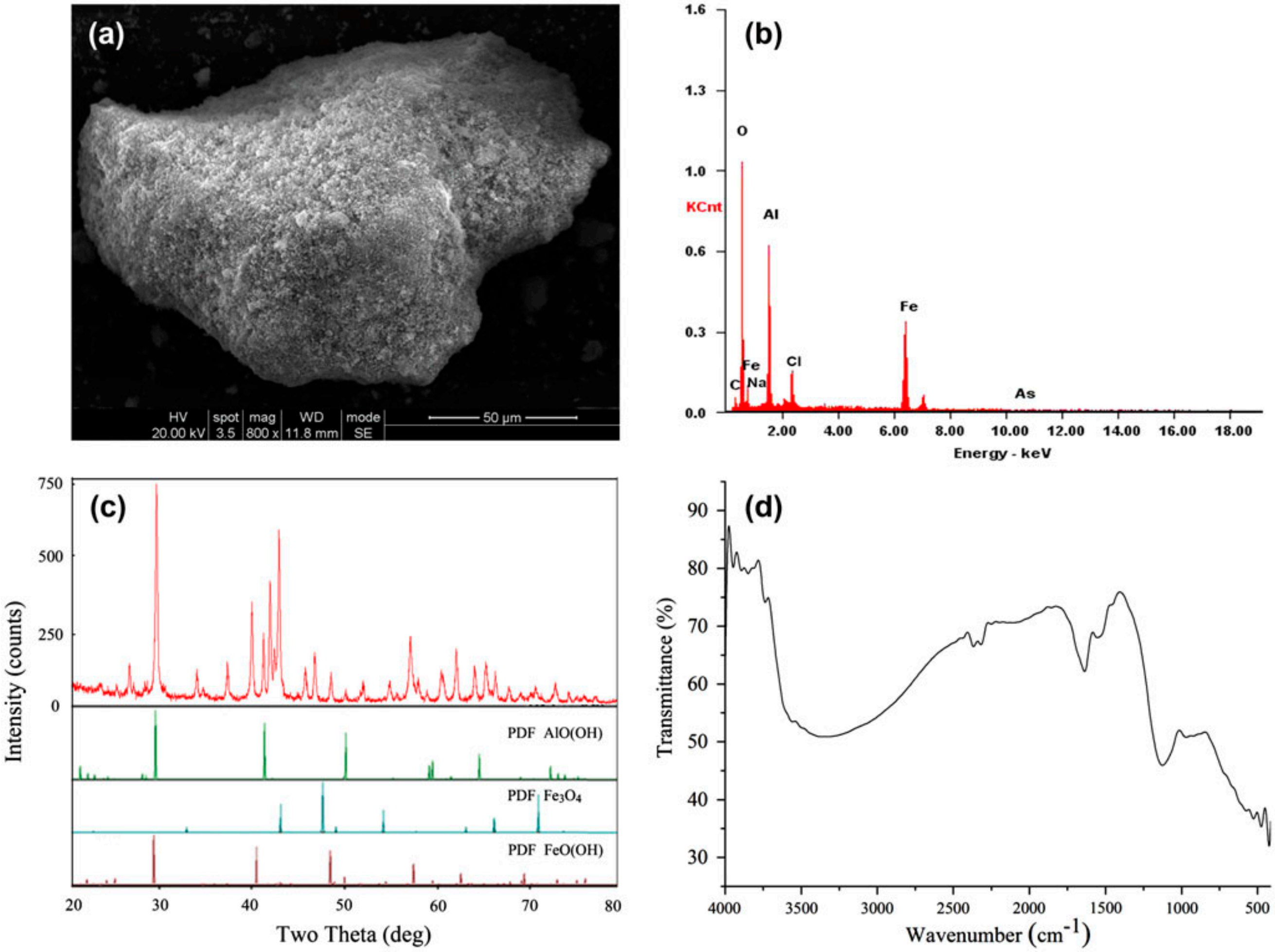

Fig. 2. SEM (a), EDS (b), XRD, (c) and FTIR (d) analysis of EC products.

but amorphous or poorly crystalline phases such as lepidocrocite (FeO(OH)), diaspora (AlO(OH)) and crystalline phases typically magnetite (Fe_3O_4) were formed in EC products, which was in agreement with other reports [27,32]. To investigate whether inclusion or occlusion is a functional mechanism responsible for As removal by EC, the degree of As removal by EC using hybrid Fe–Al electrodes was compared to adsorptive removal of As with preformed EC products which were collected by treating distilled water instead of As solutions by EC under the same conditions. Results showed that 99.58% of As were removed by EC, while with

Table 5
FT-IR vibrations, corresponding wavenumbers and ranges for the bands observed [20,33]

Type of vibrations	Vibration wavenumbers (cm^{-1})	Vibration range (cm^{-1})
OH stretching for basic hydroxyl groups from aluminum hydroxide/oxyhydroxides	3,737, 3,563	3,530–3,644
OH stretchings for hydroxyl groups from iron oxyhydroxides	3,487	3,000–3,550
Hydroxyl bending	1,638	1,572–1,813
γ´ (OH) water bending	1,638	1,572–1,813
Overtones of hydroxyl bending	1,638	1,572–1,813
	1,576	1,572–1,813
Lepidocrocite	1,131	1,090–1,245
	737	730–790
Magnetite	577, 528	526–840
Fe–O	474, 423	416–510
Al–O–H bending	975	880–1,000

performed EC product, 85.63% of As were removed, which was consistent with the results reported by Song [34]. Therefore, inclusion or occlusion seemed not to be a predominant mechanism, but adsorption onto iron and aluminum hydroxides/oxyhydroxides could be an operative removal mechanism.

4. Conclusions

In this study, experiments results revealed that RSM was a suitable method to optimize the operating conditions of EC for As removal. The response surface models developed in this study for predicting As-removal efficiency were considered to be adequately applicable. The optimum results of 99.94% As-removal efficiency and the minimum value of voltage were obtained at current density 0.47 A/dm^2, pH 7.0, aeration intensity 0.32 L/min, and operating time 20 min. Besides, SEM/EDS, XRD, and FTIR analysis of EC products revealed that adsorption onto iron and aluminum hydroxides/oxyhydroxides was the main mechanism of As removal.

Acknowledgments

We are grateful for the financial support of the National Natural Science Foundation of China (50478053), the National Key Science and Technology Project for Water Environmental Pollution Control (2009ZX07212-001-02).

References

[1] P. Ravenscroft, H. Brammer, K. Richards, Arsenic Pollution: A Global Synthesis RGS-IBG Book Series, Wiley, London, 2009.
[2] N. Balasubramanian, T. Kojima, C.A. Basha, C. Srinivasakannan, Removal of arsenic from aqueous solution using electrocoagulation, J. Hazard. Mater. 167 (2009) 966–969.
[3] M. Kobya, U. Gebologlu, F. Ulu, S. Oncela, Removal of arsenic from drinking water by the electrocoagulation using Fe and Al electrodes, Electrochim. Acta 56 (2011) 5060–5070.
[4] A.H. Smith, G. Marshall, Y. Yuan, Increased mortality from lung cancer and bronchiectasis in young adults after exposure to arsenic in utero and in early childhood, Environ. Health Persp. 114 (2006) 1293–1296.
[5] WHO (World Health Organization), Guidelines for drinking water quality: First addendum to volume 1, Recommendations, World Health Organization, Geneva, 2006.
[6] USEPA (US Environmental Protection Agency), Drinking Water Standard for Arsenic, EPA-815-F-00-015, U.S. Government Printing Office, Washington, DC, 2001.
[7] I. Ali, New generation adsorbents for water treatment, Chem. Rev. 112 (2012) 5073–5091.
[8] I. Ali, Water treatment by adsorption columns: Evaluation at ground level, Sep. Purif. Rev. 43 (2014) 175–205.
[9] S. Shevade, R.G. Ford, Use of synthetic zeolite for arsenate removal from pollutant water, Water Res. 38 (2004) 3197–3204.
[10] I. Ali, The quest for active carbon adsorbent substitutes: Inexpensive adsorbents for toxic metal ions removal from wastewater, Sep. Purif. Rev. 39 (2010) 95–171.
[11] I. Ali, M. Asim, T.A. Khan, Low cost adsorbents for removal of organic pollutants from wastewater, J. Environ. Manag. 113 (2012) 170–183.
[12] S.R. Wickramasinghe, B. Han, J. Zimbron, Z. Shen, M.N. Karim, Arsenic removal by coagulation and filtration: Comparison of ground waters from the United States and Bangladesh, Desalination 169 (2004) 231–244.
[13] I. Katsoyiannis, A. Zouboulis, H. Althoff, H. Bartel, As (III) removal from groundwaters using fixed bed upflow bioreactors, Chemosphere 47 (2002) 325–332.

[14] D. Lakshmanan, D.A. Clifford, G. Samanta, Comparative study of arsenic removal by iron using electrocoagulation and chemical coagulation, Water Res. 44 (2010) 5641–5652.

[15] M. Kobya, A. Akyol, E. Demirbas, M.S. Oncel, Removal of arsenic from drinking water by batch and continuous electrocoagulation processes using hybrid Al-Fe plate electrodes, Environ. Prog. Sustain. 33 (2014) 131–140.

[16] M. Kobya, O.T. Can, M. Bayramoglu, Treatment of textile wastewaters by electrocoagulation using iron and aluminum electrodes, J. Hazard. Mater. 100 (2003) 163–178.

[17] X.M. Chen, G.H. Chen, P.L. Yue, Separation of pollutants from restaurant wastewater by electrocoagulation, Sep. Purif. Technol. 19 (2000) 65–76.

[18] F. Akbal, S. Camci, Copper, chromium and nickel removal from metal plating wastewater by electrocoagulation, Desalination 269 (2011) 214–222.

[19] I. Ali, T.A. Khan, M. Asim, Removal of arsenic from water by electrocoagulation and electrodialysis techniques, Sep. Purif. Rev. 40 (2011) 25–42.

[20] J.A.G. Gomes, P. Daida, M. Kesmez, M. Weir, H. Moreno, J.R. Parga, G. Irwin, H. McWhinney, T. Grady, E. Peterson, D.L. Cocke, Arsenic removal by electrocoagulation using combined Al-Fe electrode system and characterization of products, J. Hazard. Mater. 139 (2007) 220–231.

[21] I. Ali, M. Asim, T.A. Khan, Arsenite removal from water by electrocoagulation on zinc-zinc and copper-copper electrodes, Int. J. Environ. Sci. Technol. 10 (2013) 377–384.

[22] I. Ali, T.A. Khan, M. Asim, Removal of arsenate from groundwater by electrocoagulation method, Environ. Sci. Pollut. Res. 19 (2012) 1668–1676.

[23] P.P. Song, Z.H. Yang, H.Y. Xu, J. Huang, X. Yang, L.K. Wang, Investigation of influencing factors and mechanism of antimony and arsenic removal by electrocoagulation using Fe-Al electrodes, Ind. Eng. Chem. Res. 53 (2014) 12911–12919.

[24] M. Kobya, E. Demirbas, U. Gebologlu, M.S. Oncel, Y. Yildirim, Optimization of arsenic removal from drinking water by electrocoagulation batch process using response surface methodology, Desalin. Water Treat. 51 (2013) 6676–6687.

[25] T. Ölmez, The optimization of Cr(VI) reduction and removal by electrocoagulation using response surface methodology, J. Hazard. Mater. 162 (2009) 1371–1378.

[26] CEPA (China Environmental Protection Agency), Water and Wastewater Monitoring Analysis Method Editorial Board, Monitoring and Analysis Methods of Water and Wastewater, fourth ed., China Environmental Science, Beijing, 2002.

[27] W. Wan, T.J. Pepping, T. Banerji, Effects of water chemistry on arsenic removal from drinking water by electrocoagulation, Water Res. 45 (2011) 384–392.

[28] M.H. Isa, E.H. Ezechi, Z. Ahmed, S.F. Magram, S.R.M. Kutty, Boron removal by electrocoagulation and recovery, Water Res. 51 (2014) 113–123.

[29] P.R. Kumar, S. Chaudhari, K.C. Khilar, S.P. Mahajan, Removal of arsenic from water by electrocoagulation, Chemosphere 55 (2004) 1245–1252.

[30] S. Amrose, A. Gadgil, V. Srinivasan, K. Kowolik, M. Muller, J. Huang, R. Kostecki, Arsenic removal from groundwater using iron electrocoagulation: Effect of charge dosage rate, J. Environ. Sci. Health A 48 (2013) 1019–1030.

[31] X.J. Guo, Z.J. Wu, M.C. He, Removal of antimony(V) and antimony(III) from drinking water by coagulation-flocculation-sedimentation(CFS), Water Res. 43 (2009) 4327–4335.

[32] M. Kang, T. Kamei, Y. Magara, Comparing polyaluminum chloride and ferric chloride for antimony removal, Water Res. 37 (2003) 4171–4179.

[33] U. Schwertmann, R.M. Cornell, Iron Oxides in the Laboratory: Preparation and Characterization, second ed., VCH, Germany, 2000.

[34] S. Song, A. Lopez-Valdivieso, D.J. Hernandez-Campos, C. Peng, M.G. Monroy-Fernandez, I. Razo-Soto, Arsenic removal from high-arsenic water by enhanced coagulation with ferric ions and coarse calcite, Water Res. 40 (2006) 364–371.